

Familial Autonomic Ganglionopathy Caused by Rare *CHRNA3* Genetic Variants

Cyndya A. Shibao, MD, Karen Joos, MD, PhD, John A. Phillips III, MD, Joy Cogan, PhD, John H. Newman, MD, Rizwan Hamid, MD, Jens Meiler, PhD, John Capra, PhD, Jonathan Sheehan, PhD, Francesco Vetrini, PhD, Yaping Yang, PhD, Bonnie Black, RN, André Diedrich, MD, PhD, David Roberston, MD, and Italo Biaggioni, MD

Correspondence

Dr. Shibao
cyndya.shibao@vumc.org

Neurology® 2021;97:e145-e155. doi:10.1212/WNL.0000000000012143

Abstract

Objective

To determine the molecular basis of a new monogenetic recessive disorder that results in familial autonomic ganglionopathy with diffuse autonomic failure.

Methods

Two adult siblings from one family (I-4 and I-5) and another participant from a second family (II-3) presented with severe neurogenic orthostatic hypotension (nOH), small nonreactive pupils, and constipation. All 3 affected members had low norepinephrine levels and diffuse panautonomic failure.

Results

Whole exome sequencing of DNA from I-4 and I-5 showed compound heterozygosity for c.907_908delCT (p.L303Dfs*115)/c.688 G>A (p.D230N) pathologic variants in the acetylcholine receptor, neuronal nicotinic, $\alpha 3$ subunit gene (*CHRNA3*). II-3 from the second family was homozygous for the same frameshift (fs) variant (p.L303Dfs*115//p.L303Dfs*115). *CHRNA3* encodes a critical subunit of the nicotinic acetylcholine receptors (nAChRs) responsible for fast synaptic transmission in the autonomic ganglia. The fs variant is clearly pathogenic and the p.D230N variant is predicted to be damaging (SIFT)/probably damaging (PolyPhen2). The p.D230N variant lies on the interface between *CHRNA3* and other nAChR subunits based on structural modeling and is predicted to destabilize the nAChR pentameric complex.

Conclusions

We report a novel genetic disease that affected 3 individuals from 2 unrelated families who presented with severe nOH, miosis, and constipation. These patients had rare pathologic variants in the *CHRNA3* gene that cosegregate with and are predicted to be the likely cause of their diffuse panautonomic failure.

From the Department of Medicine (C.S., J.H.N., B.B., A.D., D.R., I.B.), Department of Ophthalmology and Visual Sciences, Biomedical Engineering (K.J.), Department of Pediatrics (J.A.P., J.C., R.H.), and Department of Biochemistry (J.M., J.C.), Vanderbilt University Medical Center, Nashville, TN; Department of Internal Medicine (J.S.), Washington University in St. Louis, MO; Department of Medical and Molecular Genetics (F.V.), Indiana University School of Medicine, Indianapolis, IN; and Baylor Genetics and Baylor College of Medicine (Y.Y.), Baylor College of Medicine, Houston, TX.

Go to [Neurology.org/N](https://www.neurology.org/N) for full disclosures. Funding information and disclosures deemed relevant by the authors, if any, are provided at the end of the article.

Glossary

BP = blood pressure; CNV = copy number variant; DBH = dopamine β -hydroxylase; DHPG = dihydroxyphenylglycol; HF = high-frequency; HF_{rrt} = high-frequency heart rate variability; HR = heart rate; LF = low-frequency; LF_{sbp} = low-frequency systolic blood pressure; nAChR = nicotinic acetylcholine receptor; nOH = neurogenic orthostatic hypotension; PNS = parasympathetic nervous system; PRT = prolonged blood pressure recovery time; RRI = R-R interval; SNS = sympathetic nervous system; UDN = Undiagnosed Diseases Network; WES = whole exome sequencing.

The CHRNA3 subunit of the nicotinic acetylcholine receptor (nAChR α 3) plays a crucial role in the autonomic function of multiple organs. This subunit forms heteromultimeric nAChRs with other subunits, most frequently α 3 β 4, also known as the “ganglia-type” nAChRs.¹ The nAChR α 3 subunit is primarily located in the autonomic ganglia, and is also found in the interpeduncular nucleus and medial habenula, which modulate nicotine addiction,^{2,3} pineal gland,^{2,4} superior colliculi,² cerebellum,^{2,5} and peptidergic C-fiber nociceptor subset mediated by nerve growth factor.⁶

nAChR α 3 is directly involved in ganglionic synaptic transmission as a predominant ligand-binding subunit, mediating both monovalent and Ca²⁺ conductances increase in response to acetylcholine and nicotinic agonists. Autonomic ganglia neurotransmission is critical for the stimulation of sympathetic nervous system (SNS) and parasympathetic nervous system (PNS) neural pathways that regulate blood pressure (BP) upon standing, providing adrenergic signals for vasoconstriction.

Nowhere is the importance of this system more evident than in patients with autoimmune autonomic ganglionopathy; these patients develop antibodies against nAChRs found in their serum, particularly nAChR α 3, and develop diffuse autonomic failure characterized by significant neurogenic orthostatic hypotension (nOH) and gastrointestinal disturbances.^{7,8} Moreover, lack of in situ hybridization or immunocytochemistry detection of nAChR α 3 in surgical samples was reported in the rare infantile fatal megacystis-microcolon-intestinal hypoperistalsis syndrome (MMIHS).⁹ Conversely, 3 different homozygous mutations in nAChR α 3 were recently said to cause significant congenital renal and bladder anomalies, and impaired pupillary reflex, but otherwise asymptomatic.¹⁰ The critical role the nAChR α 3 subunit plays on autonomic function was also demonstrated by the development of autonomic dysfunction in mice that have been genetically modified to lack the *CHRNA3* gene.¹¹

We report a novel genetic disease caused by compound heterozygous and homozygous variants in the *CHRNA3* gene that encodes the nAChR α 3 subunit. This condition, which we named familial autonomic ganglionopathy, affected 3 individuals from 2 unrelated families, all of whom are presented with diffuse panautonomic failure characterized by severe nOH, constipation, and miosis with poorly reactive pupils and peripheral radial transillumination defects in the dilator muscle area.

Methods

The families' pedigrees are presented in figure 1. Patients I-4 and I-5 were referred to the Vanderbilt Autonomic Dysfunction Center for evaluation in 1995. They were admitted to the General Clinical Research Center at Vanderbilt University Medical Center for a comprehensive assessment of their autonomic function. These patients were later referred to the Undiagnosed Diseases Network (UDN) for genetic evaluation, and when the mutation was discovered, reexamined in early 2019.

Subject II-3 was identified through the GeneMatcher web-based tool,¹² and was admitted in the fall of 2019 to our center for autonomic phenotyping. Medications with cardiovascular/autonomic effects were discontinued for ≥ 5 half-lives before admission. Evaluation consisted of a comprehensive medical history, physical examination, 12-lead ECG, laboratory assessments, ophthalmic examination with available ancillary tests and standard autonomic tests, along with pharmacologic evaluation as described in the following paragraphs. Every effort was made to obtain medical records from outside hospital facilities.

Standard Protocol Approvals, Registrations, and Patient Consents

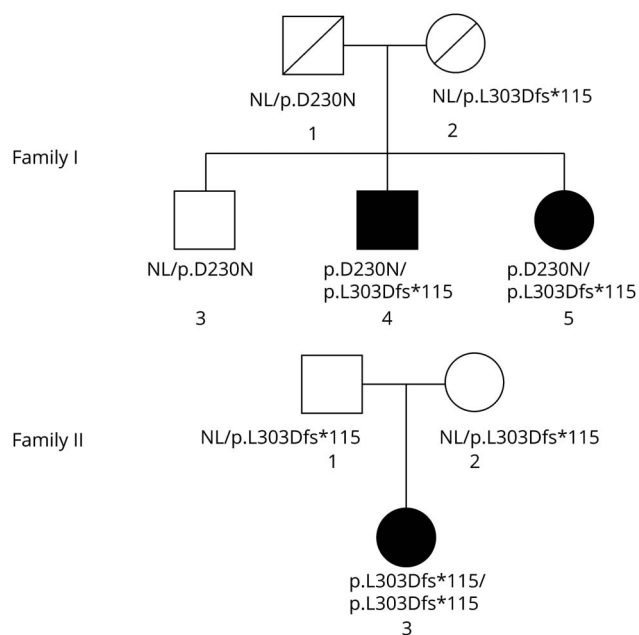
Written informed consents were obtained from patients I-4 and I-5 as well as II-3's legal guardian and the following study protocols were used: clinicaltrials.gov NCT00338065, NCT02450851, and NCT00338065. They were approved by the Vanderbilt Institutional Review Board and conducted under the tenets of the Declaration of Helsinki.

The present study is neither a clinical trial nor an observational study. Therefore, the *New England Journal of Medicine* guidelines for statistical reporting do not apply. We report the in-depth phenotyping of a condition known as familial autonomic ganglionopathy affecting 3 individuals and a statistical analysis was not performed.

Autonomic Cardiovascular Evaluation

Standardized autonomic function tests were performed to assess the severity of autonomic impairment including an orthostatic stress test, Valsalva maneuver, and cold pressor test to assess cardiovascular autonomic function. Sinus arrhythmia monitoring during controlled breathing was used to assess cardiac parasympathetic activity.^{13,14} BP and heart rate (HR) during all of these tests were obtained using an

Figure 1 Families' Pedigrees



The pedigree structure of the 2 families (family I and family II); affected individuals are shown as filled symbols, on which complete sequencing analysis was performed and a pathogenic *CHRNA3* genetic variant was found.

automated sphygmomanometer (Dinamap, GE Medical Systems Information Technologies) and noninvasive continuous BP monitoring (Finapres Medical System).

Spectral Analysis of BP and HR

Spectral analyses of BP and HR were obtained to evaluate for sympathetic and parasympathetic function. Hemodynamic data were recorded using the WINDAQ data acquisition system (DI720, DATAQ; 14 Bit, 1000 Hz) and were processed offline using custom written software in PV-Wave language (PV-wave, Visual Numerics Inc.). Detected beat-to-beat values of R-R intervals (RRI) and BP were interpolated and low-pass filtered (cutoff 2 Hz). Data segments of at least 180 seconds were used for spectral analysis. Linear trends were removed and power spectral density was estimated with the FFT-based Welch algorithm. The total power and the power in the low-frequency (LF: 0.04 to <0.15 Hz) and high-frequency (HF: 0.15 to <0.40 Hz) ranges were calculated according to the previously described methods by Diedrich et al.¹⁵

Phenylephrine Test

The study was conducted in a quiet thermoneutral environment with the patient resting supine on a hospital bed. Incremental boluses of phenylephrine, an α 1 adrenergic agonist (Hikma Pharmaceuticals), were infused into an antecubital intravenous catheter in patients I-4 and I-5, starting with a dose of 12.5 μ g until BP increased 25 mm Hg. Continuous BP and HR were monitored with a noninvasive continuous BP monitoring system.

Tyramine Infusion Test

Tyramine releases norepinephrine from sympathetic nerve endings if there is normal norepinephrine reuptake and storage. The brother (I-3, healthy control) and affected male patient (I-4) received incremental doses of tyramine (Spectrum Chemical) from 250 up to 4,000 μ g at 10- to 15-minute intervals through an intravenous catheter. Throughout, continuous BP was monitored with an intra-arterial line and a noninvasive continuous BP monitoring system.

Pyridostigmine Test

The study was conducted in the morning, 2.5 hours after a meal to avoid postprandial hypotension. Baseline BP and HR were measured every 5 minutes with an automated brachial BP cuff while participants were seated on a chair with their feet on the floor for 30 minutes, then BP and HR were obtained while standing at 1, 3, 5, and 10 minutes as a measurement of orthostatic tolerance. Subsequently, a 60-mg pyridostigmine tablet (Valeant Pharmaceuticals International) was administered and sitting BP and HR were likewise measured for 60 minutes. Orthostatic tolerance was assessed at the end of this period.

Neurohormonal Assessment

Plasma samples were collected with participants in supine and upright postures through an IV catheter placed >30 minutes before sampling. Catecholamines (DHPG, dihydroxyphenylacetic acid, norepinephrine, epinephrine, and dopamine) were quantified using high-performance liquid chromatography with electrochemical detection as previously described.¹⁶

Whole Exome Sequencing

Both affected siblings (I-4, I-5) were referred to the UDN (clinicaltrials.gov; NCT02450851). They were enrolled at the Vanderbilt clinical site, and consented to the study (institutional review board protocol NHGRI 15-HG0130) before any genetic studies were carried out. Following the patients' enrollment, clinical whole exome sequencing (WES) analysis was completed at the UDN in the Exome Laboratory at Baylor Genetics and the sequencing and data analyses were conducted as previously described.¹⁷ Samples were also analyzed by cSNP array (Illumina HumanExome-12 v1 array) for quality control assessment of exome data, as well as for detecting large copy number variants (CNVs) and regions of absence of heterozygosity.¹⁷ The 3 CNV deletions were detected using customized exon-targeted oligo arrays (Oligo V8, V9, and V10) designed at Baylor Genetics,¹⁸ which cover more than 4,800 known or candidate disease genes with exon level resolution. The WES-targeted regions cover >23,000 genes for capture design (VCRome by NimbleGen), including the coding and the untranslated region exons. The mean coverage of target bases was >140 \times and >96% of target bases were covered at >20 \times .¹⁷

GnomAD and ExAC databases were used to determine the frequency of the variants in the normal population (gnomad.broadinstitute.org/gene/ENSG00000080644?dataset=gnomad_r2_1; accessed May 5, 2020). Polyphen2 (genetics.bwh.harvard.edu/pph2/) and SIFT (sift.bii.a-star.edu.sg/) were used to predict

Table 1 Autonomic Function Testing and Neurohormonal Assessment

Autonomic testing	I-4	I-5	II-3	Normal values
Orthostatic test				
Orthostatic change in SBP, mm Hg	-58	-26	-34	<20
Orthostatic change in HR, bpm	10	30	-7	>10
Sinus arrhythmia, SA ratio	1.02	1.16	1.3	1.2 ± 0.1
Valsalva maneuver				
Depressor response, phase II, mm Hg	-20	-55	7	<20
Pressor response, phase II, mm Hg	-4	Absent	Absent	>10
Valsalva ratio	1.02	1	2.2	>1.4
BP recovery time, s	23	21	29	1 ± 1.98
Hyperventilation, depressor response, mm Hg	-39	-26	-4	<10
Handgrip, pressor response, mm Hg	2	6	12	>20
Cold pressor, pressor response, mm Hg	7	108	138	>20
Catecholamines				
DHPG, pg/mL^{8,18}				
Supine	520	737	462	1,292 ± 113
Upright	504	706	Absent	
Norepinephrine, pg/mL				
Supine	41	71	80	210 ± 11
Upright	58	127		443 ± 47
Epinephrine, pg/mL				
Supine	4	35	5	29 ± 9
Upright	12	37	Absent	42 ± 12
Dopamine, pg/mL				
Supine	19	39	<3	55 ± 16
Upright	37	57	Absent	61 ± 13

Abbreviations: BP = blood pressure; DHPG = dihydroxyphenylglycol; HR = heart rate; SBP = systolic blood pressure. Data available from Dryad (table e-1, Neural Pathways of Autonomic Reflexes in Familial Autonomic Ganglionopathy; tables e-1A and e-1B, Eye Examination Results; doi.org/10.5061/dryad.xgxd254fg).

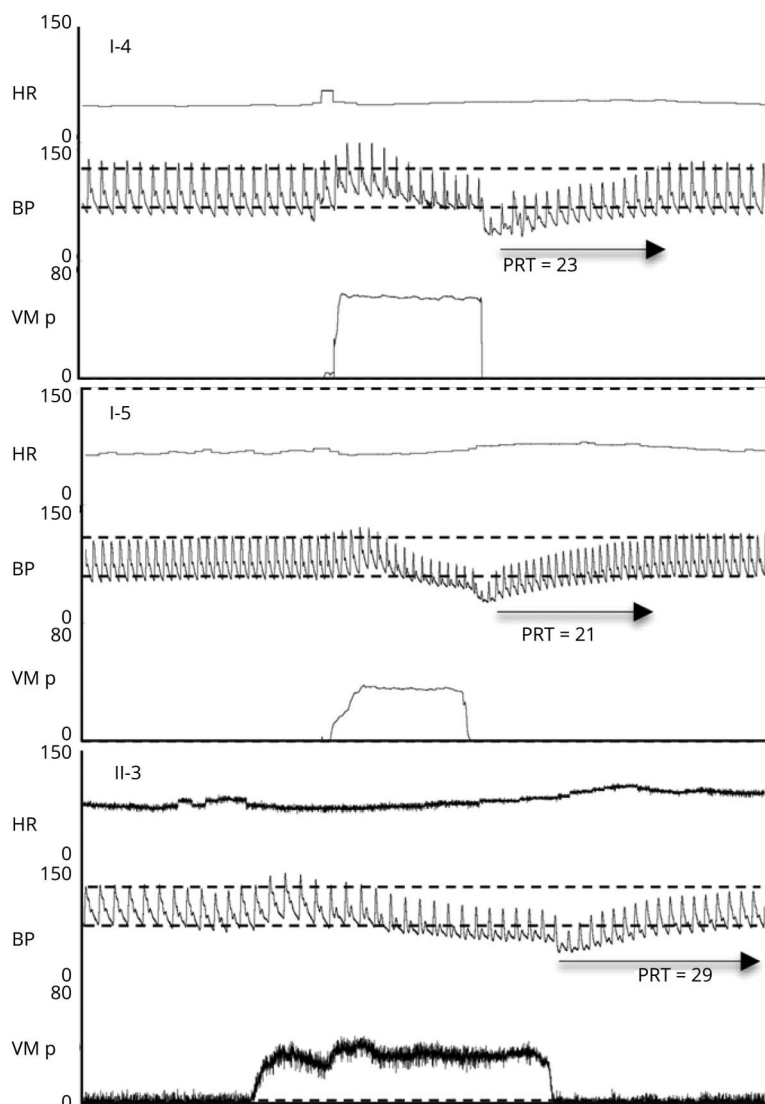
the functional impact of the genomic variants leading to amino acid substitutions. The WES analysis for the affected patient from the second family (II-3) was completed at GENE DX following published standard approaches. Accordingly, the gene variant was submitted to GeneMatcher.¹²

α3β4 nAChR Cryo-EM Structure

The 3.8 Ångstrom resolution cryo-EM structure (PDB code 6PV8) of the ligand-bound human α3β4 nAChR¹⁹ was used to predict the effects of the D230N variant on the protein structure. Thermodynamic destabilization by the D230N variant was predicted using Rosetta's ddG_monomer application, which calculates energy scores for the structure before and after mutation, thus allowing repacking of

sidechains without backbone movement.²⁰ Owing to the fact that the model was not a high-resolution X-ray crystal structure, the low-resolution protocol was used, corresponding to row 3 of table 1 from Kellogg et al.²⁰ In order to compare the location of the D230N variant to the spatial distributions of known benign vs disease-associated variants, the PathProx algorithm^{21,22} was employed to map known ExAC and ClinVar missense variants to the structure and calculate a proximity score. However, this calculation was not completed due to a lack of disease-associated variants. In addition, structural measurements and analysis, along with molecular graphics, were generated using UCSF Chimera²³ (supported by NIH P41 RR-01081) as distributed by SBGRID.²⁴

Figure 2 Valsalva Maneuver Tracings



Continuous heart rate (upper channel), blood pressure (middle channel), and pressure (third channel during Valsalva maneuver) in all affected individuals (I-4, I-5, II-3). Valsalva maneuver pressures were between 30 and 40 mm Hg in all 3 individuals.

Data Availability

Any anonymized data not published within the article will be shared by request from any qualified investigator.

Results

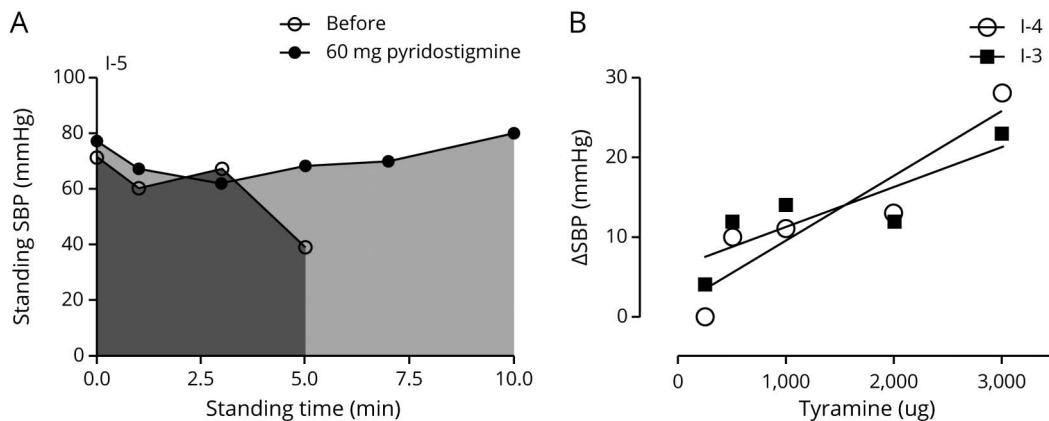
Clinical Characteristics

The families' pedigrees are shown in figure 1. In family I, the affected male proband (I-4) was referred to our center for evaluation regarding episodes of postural dizziness, blurred vision, weakness, nausea, constipation, and excessive fatigue. His symptoms started during childhood, and at age 39 years he had become disabled. His lightheadedness worsened upon standing and after large meals. In addition, he smoked 3 packs per day beginning at age 16, which alleviated his symptoms, albeit subjectively. However, after developing a smoker's cough at age 27, he stopped smoking and subsequently developed worsening autonomic symptoms. He had no history of developmental delay

and, despite exhibiting moderate urinary symptoms with an American Urological Association Score Questionnaire symptom of 9, the urodynamic study showed normal urinary flow rate with no hyporeflexia, the bladder neck was closed at all times, and the Valsalva leak pressure was >100 cm H₂O.

The female patient I-5 was 3 years younger than I-4. Her symptoms included postural dizziness and lightheadedness; her first syncopal episode occurred at age 13. As with patient I-4, she had no history of developmental delay. I-5 reported severe constipation throughout her life, as well as worsened postural lightheadedness after eating large meals and during her pregnancies. Unlike I-1 through I-4, she did not smoke; she developed urinary retention in her mid-40s, with a post-void residual volume of 230 mL of urine. A urodynamic test was not performed on her.

Both siblings had no history of epilepsy and had normal neurologic examinations. I-4 had retrograde ejaculation, I-5



(A) Effect of 60 mg pyridostigmine on standing systolic blood pressure (SBP) and time in I-5. (B) I-3 and I-4 had a normal pressor response to tyramine, which indicated preserved sympathetic postganglionic neurons.

had intact sexual function, and all their offspring were healthy. The siblings have an older brother (I-3) who was healthy and did not smoke; both parents (I-1, I-2) had hypertension; I-1 did not smoke, I-2 used to smoke for 25 years, but then stopped; they both died in their late 80s.

The affected patient from the second family is a 15-year-old girl (II-3); she was the product of a normal, full-term pregnancy without complications during delivery. Despite the healthy and routine pregnancy, during her infancy, she developed severe constipation that resulted in multiple emergency visits due to fecal impaction. At 5 months of age, her mother noted small pupils. During her early childhood, the patient had difficulties walking at a fast pace and was not able to participate in sports due to fatigue. At age 5, she had learning difficulties while attending kindergarten. During this time, she complained of blurred vision and light sensitivity and was diagnosed with an iris transillumination defect during an ophthalmologic examination. At age 13, she underwent a formal psychological evaluation, and was diagnosed with mild intellectual disabilities; her Wechsler Intelligence Scale for Children (WISC-V) IQ was very low at 72 (average 90–109). She had no history of epilepsy; MRI of her brain, with and without contrast, was normal. She has an older half-brother who completed high school without difficulties and her mother and father were healthy.

Autonomic Phenotype

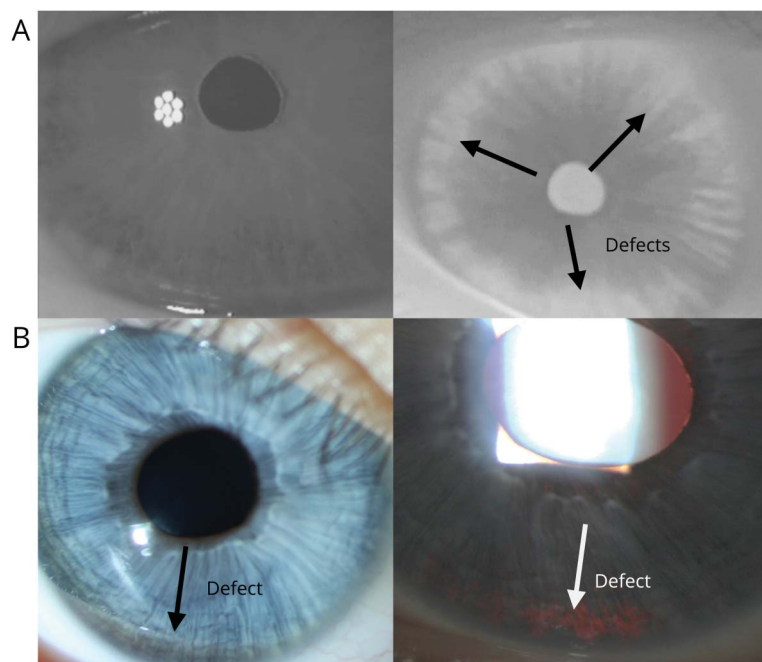
Family I

The proband (I-4) and his sister (I-5) had severe nOH; patient I-4's orthostatic vital signs were supine BP 120/80 mm Hg, HR 48 bpm and standing BP 52/36 mm Hg, HR 65 bpm. Patient I-5's orthostatic vital signs were supine BP 114/74 mm Hg, HR 65 bpm and standing BP 88/66 mm Hg, HR 95 bpm. Patient I-5 had a greater compensatory HR response on standing (table 1). Orthostatic vital signs obtained in patients I-1, I-2, I-3, and I-

4's 3 biological children and I-5's children were negative for nOH. I-4 had impaired cardiovagal response with a blunted sinus arrhythmia, whereas I-5 had a mild cardiovagal impairment (table 1). I-4 and I-5 had impaired sympathetic vasoconstrictor response with abnormal Valsalva maneuver and prolonged BP recovery time (PRT) (23 and 21 seconds, respectively; normal value, 1 ± 1.98 seconds), which indicated impaired sympathetic vasoconstrictor activity (figure 2). Both I-4 and I-5 also had an abnormal decrease in BP during hyperventilation and blunted increase in BP during the cold pressor test and the handgrip test (table 1). Spectral analysis of BP and HR showed that both I-4 and I-5 had severely reduced sympathetic activity with LF systolic BP (LF_{sbp}) 1.44 and 1.80 mm Hg², respectively, the age-matched normal value being 5.5 ± 1.09 mm Hg^{2.25}. Of note, I-4 had decreased PNS activity and HF HR variability (HF_{rri}) 13.9 ms², whereas subject I-5 had some preservation of PNS activity (HF_{rri} 134.5 ms²), age-matched normal value being 175.3 ± 51.42 ms².

I-5 received a single dose of 60 mg of pyridostigmine, an acetylcholinesterase agent that increases the availability of acetylcholine in the synapse. Accordingly, this patient showed an improvement in standing systolic BP from 40 to 80 mm Hg, standing time from 5 to 10 minutes, and presyncopal symptoms (figure 3A). The proband (I-4) and his healthy brother (I-3) had a normal BP response to tyramine, displaying little change with doses below 2000 μ g; the BP increased >20 mm Hg with doses of 3,000 μ g and higher, which is a normal response (figure 3B). The normal pressor response to tyramine in I-4 indicated that sympathetic neurons were spared.¹³ I-4 and I-5 had an increase of 25–30 mm Hg with 25 μ g of phenylephrine consistent with hypersensitivity of $\alpha 1$ adrenergic receptors (data available from Dryad, table e-1, doi.org/10.5061/dryad.xgxd254fg).

I-4 and I-5 had abnormally low levels of norepinephrine while supine (41 and 71 pg/mL, respectively; normal value, 210 \pm



Ophthalmologic evaluation showed peripheral transillumination iris defects in I-5 with infrared image (A) and II-3 with standard clinical slit lamp (B).

11 pg/mL)²⁶ and while standing (58 and 127 pg/mL, respectively; normal value, 443 ± 47 pg/mL), confirming impaired sympathetic activation. Dihydroxyphenylglycol (DHPG),¹⁶ a marker of neuronal metabolism of norepinephrine, was also decreased. The levels of dopamine were normal, indicating that enzymatic conversion of dopamine to norepinephrine was preserved (table 1).

Family II

II-3's orthostatic vital signs were BP 120/68 mm Hg, HR 99 bpm supine and BP 86/50 mm Hg, HR 92 bpm standing after 3 minutes. Autonomic function testing showed a blunted sinus arrhythmia (1.19) and impaired sympathetic vasoconstrictor response with no pressor effect during phase II late and phase IV of the Valsalva maneuver (table 1). This patient had a prolonged PRT (29 seconds; normal value, 1 ± 1.98 seconds) (figure 2).

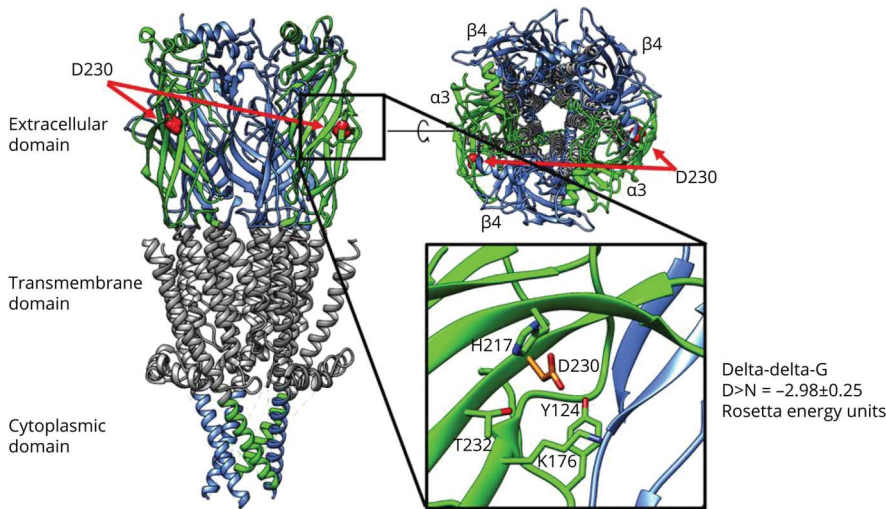
Spectral analysis of BP and HR showed that II-3 has severely impaired SNS activity (LF_{sbp} 1.2 mm Hg²; normal value, 5.5 ± 1.09 mm Hg² and PNS activity (HF_{rrt} 200.4 ms²; age-matched normal value, 1,130 ± 103.8 ms²).²⁷ Like I-1 and I-2, II-3 had very low plasma norepinephrine while supine (80 pg/mL; normal value, 210 ± 11 pg/mL). The participant declined standing catecholamine level sampling (table 1). These results showed severe and diffuse autonomic failure.

Ocular Phenotype

The ocular examination results from 1995 to 2019 are summarized in tables e-2A and e-2B (doi.org/10.5061/dryad.xgxd254fg; data available from Dryad). Compared to their

unaffected brother (I-3), I-4 and I-5 reported blurred vision while standing and dry eyes. They had lightly colored irides, miosis with poorly reactive pupils, peripheral radial transillumination defects in the dilator muscle area, and bilateral ptosis. In addition, I-5 had iris sphincter translucency identified by an infrared camera (figure 4A). I-5 was monocular right due to left eye enucleation for retinoblastoma at age 2 years. II-3 from the second family also complained about blurred vision and vague eye pain. She was locally clinically diagnosed with albinism/albinoidism due to her blue irides and transillumination defects (figure 4B). All 3 affected patients had no Krukenberg spindle and no backward bowing of the iris; I-4 and I-5 had normal trabecular meshwork pigmentation (II-3 declined gonioscopy), indicating no pigment dispersion syndrome. All 3 participants had very limited light–dark responses. Normal participant I-3 dilated with 10% cocaine, whereas both I-4 and I-5 had no reaction (data available from Dryad; table e-2A, doi.org/10.5061/dryad.xgxd254fg). Cocaine was not available for testing II-4. Interestingly, 1% hydroxyamphetamine caused dilation in I-5, whereas no reaction occurred in I-4. It is not known whether this was due to his markedly unresponsive pupils. Instillation of 1% apraclonidine OD resulted in a slightly increased OD pupil size and elevation of the right eyelid in all 3 affected participants (data available from Dryad; table e-2B, doi.org/10.5061/dryad.xgxd254fg). Mild ptosis reversal is consistent with sympathetic loss because the Muller muscle that assists the elevation in the upper eyelid has sympathetic innervation. Moreover, reduced basal tear production by Schirmer test with proparacaine after 5 minutes was found in all 3 affected participants, especially in II-3, who complained of ocular

Figure 5 Model of Nicotinic Acetylcholine Receptor (nAChR) $\alpha 3\beta 4$ and D230 Variant Location



Structural effect of D230N mutation on nAChR pentameric channel. The 3.8 Å resolution cryo-EM structure (PDB code 6PV8) of the ligand-bound human $\alpha 3\beta 4$ nicotinic acetylcholine receptor is shown. The $\alpha 3$ subunits are shown in green and the $\beta 4$ subunits are blue. All transmembrane regions are gray. The location of the D230N variant is shown with red spheres to demonstrate its proximity to the inter-subunit interfaces and to the ligand binding cleft. The inset shows as sticks the neighboring residues of the native aspartic acid, highlighted here in orange. The replacement of this buried negative charge with a neutral residue will change the electrostatics of the site, which is likely to lead to a change in the dynamics of the protein by altering the interaction with the nearby lysine residue K176. Finally, the negative value of the Rosetta thermodynamic calculation predicts a hyperstabilization of the system that could also affect channel function.

discomfort (data available from Dryad; table e-2B, doi.org/10.5061/dryad.xgxd254fg). Ergo, artificial tears were recommended, with some symptomatic relief later reported. In addition, the 3 patients had marked decreases in their intraocular pressures with upright postures, which was associated with a decrease in their standing BPs (data available from Dryad; tables e-2A and e-2B, doi.org/10.5061/dryad.xgxd254fg).

Genetic Results

The UDN WES of DNAs from the proband (I-4) and his affected sibling (I-5) showed that both were compound heterozygotes for c.907_908delCT (p.L303Dfs*115)/c.688 G>A (p.D230N) variants in the *CHRNA3* (NM 000743) gene. In family I, the frameshift and missense *CHRNA3* variants were inherited from their mother (I-1) and father (I-2), respectively, and their nonaffected brother (I-3) was a nL/p.D230N heterozygote. The frameshift variant is likely to be pathogenic as it is predicted to create a premature stop codon, potentially leading to mRNA nonsense-mediated decay; the p.D230N variant is predicted to be damaging (SIFT)/probably damaging (PolyPhen2). The variant c.907_908delCT (p.L303Dfs*115) has been seen in the heterozygous state 56 times; the p.D230N, only one time in GnomAD. II-3 from family II was homozygous for the likely pathologic variant c.907_908delCT (p.L303Dfs*115)/c.907_908delCT (p.L303Dfs*115).

Modeling of the p.D230N Variant in the Pentameric Protein

Modeling the effect of the p.D230N variant in the context of the pentameric protein structure provides 3 mechanistic hypotheses to rationalize the observed phenotypes (figure 5). The Rosetta calculation of $\delta\text{-}\delta\text{-G}$ gave a negative value (-2.98 ± 0.25 Rosetta energy units, correlating roughly with kcal/mol). This predicts a thermodynamic hyperstabilization of the protein as a lowered free-energy state often correlates with altered protein dynamics, and consequently altered function.

The change happens in the extracellular domain, less than 9 Å from the interface between channel subunits, and within 10 Å of the nicotine binding site. Furthermore, the replacement of a buried, charged aspartic acid with a neutral asparagine will alter the electrostatic environment of the neighboring residues, notably lysine 176. Nonetheless, testing these hypotheses with biochemical experiments is yet to be done.

Discussion

We have discovered a novel genetic disease named familial autonomic ganglionopathy that causes severe and diffuse autonomic failure affecting 3 patients from 2 unrelated families. Patients from family I (I-4, I-5) were compound heterozygotes for c.907_908delCT (p.L303Dfs*115)/c.688 G>A (p.D230N) variants in the *CHRNA3* gene. Patient II-3 from family II was homozygous for the same pathologic fs mutation (p.L303Dfs*115/p.L303Dfs*115) found in family I. These variants are predicted to damage the function of the nAChR $\alpha 3$ subunit, which is primarily expressed in the autonomic ganglia that mediate fast synaptic transmission.

Our 3 patients associated with *CHRNA3* variants presented with diffuse panautonomic failure characterized by significant nOH, constipation, miosis, and urinary retention. In I-4 and I-5, nOH was not symptomatic until young adulthood. II-3 had a much more severe condition with symptoms during infancy and her disease was also associated with intellectual impairment. Our comprehensive autonomic evaluation revealed that all patients had significant impaired sympathetic vasoconstrictor activity. Supine norepinephrine and intraneuronal metabolite (DHPG) levels were low and failed to increase while upright; this was associated with hypersensitivity of $\alpha 1$ adrenoceptor, commonly observed in conditions

with reduction of neuronal levels of norepinephrine. Of note, even though the circulating levels of norepinephrine were low, I-4 had a normal pool of norepinephrine in the neuronal terminal because the pressor response to tyramine was normal. In light of these findings, the interpretation was that the stimulation of efferent, postganglionic sympathetic fibers and subsequent norepinephrine release and pressor response was impaired in these patients; however, the sympathetic neurons were spared. Summary data are available from Dryad (table e-1, doi.org/10.5061/dryad.xgxd254fg).

Parasympathetic nerves were also affected in I-4 and II-3; spectral analysis of HF variability confirmed that both patients had significantly low HF_{rrt} compared to age-matched normative values. HF_{rrt} in I-5 was in the low normal range, indicating preserved PNS function. Therefore, to ascertain whether increased acetylcholine, which is the main neurotransmitter in the autonomic ganglia, could improve orthostatic intolerance in I-5, an acetylcholinesterase inhibitor was administered; this drug class has been reported to alleviate nOH.²⁸ This was demonstrated when an acute administration of 60 mg pyridostigmine significantly improved I-5's standing BP and time. As such, it was considered as a potential treatment for this patient. However, I-5 decided to postpone the initiation of the treatment with pyridostigmine.

The 3 patients had a unique bilateral ocular phenotype with poorly reactive miotic pupils and ptosis with a positive response to topical apraclonidine, lightly colored irides, transillumination defects, reduced basal tear production, and intraocular pressure that decreased acutely with an upright posture. These ocular findings were consistent with autonomic impairment. A perinatal sympathetic disruption is posited to reduce the postnatal neural crest-derived melanocyte migration into the iris anterior border and stroma, causing the lightly colored irides.²⁹ Our patients presenting with the added phenotype of transillumination defects have had iris autonomic disruption since in utero development, which could represent a continued lack of sympathetic stimulus since earliest development.

The study by Xu et al.¹¹ generated *CHRNA3* mutant C57BL/6 mice with the deleted exon 5 without AChR α 3 subunit mRNA expression and reduced ACh-activated currents in the superior cervical ganglia neurons. Similar to our patients, the mice had severe ptosis consistent with sympathetic dysfunction and poorly reactive pupils. However, the mutant mouse also had megacystis with absent nicotine contraction, growth impairment, and shortened life span, which was not observed in our patients.¹¹ It could be postulated that the *CHRNA3* mutant genetics' background contributed to the different autonomic phenotypes and shortened life span. In this context, a knock-in C57BL/6 version of *CHRNA3* was similar to the knock-out, but with mild hydronephrosis and no reported megacystis. In these mice, ptosis was listed, but the pupils were not examined. When the knock-in mutation was transferred to BALB/cJ mice, growth was normal with longer life

spans.³⁰ Furthermore, the original *CHRNA3* knockout, when bred into the CD1 mouse, appeared healthier and lived longer (Edward Hawrot, personal communication); altogether, the evidence supported our hypothesis that genetic background played an important role in the different mouse autonomic phenotypes.

The same investigators also generated β 2-/ β 4-/- double mutants that survived to birth but have impaired growth and increased perinatal mortality. These 2 β subunits can form heteromultimeric channels with any of the α 2, α 3, α 4, or α 5 subunits in heterologous expression systems, and are also widely expressed in the autonomic ganglia. Similar to the *CHRNA3* knockout mouse, they were presented with autonomic compromise, including enlarged bladders and dribbling urination. These findings corroborate with the concept that genetic modifications in the subunits of the ganglia-type nAChRs shared similar, but not identical, autonomic phenotype.

Autonomic failure has been associated with other genetic diseases that disrupt the function of enzymes necessary for catecholamine metabolism.³² Among them are tetrahydrobiopterin deficiency, Menkes disease, aromatic L-amino acid decarboxylase deficiency (AAAD), monoamine oxidase deficiency, dopamine β -hydroxylase (DBH) deficiency,³³ and CYB561 deficiency.³⁴ nOH is particularly severe in DBH and CYB561 deficiencies. These patients present with syncopal episodes in their first years of life while learning to walk. In comparison, our patients with the *CHRNA3* variants had later and less severe nOH symptoms, but had evidence of other organs compromised by diffuse autonomic impairment. These differences, particularly, the iris transillumination defects in the *CHRNA3* variants, are important to recognize in order to guide appropriate confirmatory genetic testing.

We report 3 individuals from 2 unrelated families with nOH and autonomic failure who are compound heterozygotes or homozygous for *CHRNA3* variants. These variants have predicted detrimental effects on nAChR α 3 structure and function, which play a vital role in autonomic ganglionic transmission.

Acknowledgment

Contributors from the Undiagnosed Diseases Network are listed at [links.lww.com/WNL/B407]. Supported by The Lori Ann Fishel Fund, The William Black and Joseph Ellis Research Funds, and an unrestricted departmental grant from Research to Prevent Blindness. Photographers: Tony Adkins, CRA, OCT-C; Min McWilliams, COT; and Sean Donahue, MD, PhD, Department of Ophthalmology and Visual Sciences, Vanderbilt University Medical Center, Nashville, TN.

Study Funding

National Institutes of Health, The William Black and Joseph Ellis Research Funds, and an unrestricted departmental grant from Research to Prevent Blindness.

Disclosure

C.A. Shibao received speaker honorarium from Lundbeck Pharmaceuticals and consulting honoraria from Lundbeck and Theravance Biopharma. I. Biaggioni received speaker honorarium from Lundbeck Pharmaceuticals and consulting honoraria from Lundbeck and Theravance Biopharma. K. Joos, J.A. Phillips, J.D. Cogan, J.H. Newman, R. Hamid, J. Meiler, J.A. Capra, J.H. Sheehan, F. Vetrini, Y. Yang, B. Black, A. Diedrich, and D. Robertson report no disclosures relevant to the manuscript. Go to Neurology.org/N for full disclosures.

Publication History

Received by *Neurology* December 16, 2019. Accepted in final form April 8, 2021.

Appendix Authors

Name	Location	Contribution
Cyndya A. Shibao, MD	Vanderbilt University Medical Center, Nashville, TN	Clinical evaluation, literature search, figures, data collection, analysis, writing of the manuscript
Karen M. Joos, MD, PhD	Vanderbilt University Medical Center, Nashville, TN	Clinical evaluation, literature search, figures, data collection, analysis, writing of the manuscript
John A. Phillips III, MD	Vanderbilt University Medical Center, Nashville, TN	Literature search, figures, data collection, analysis, writing of the manuscript
Joy D. Cogan, PhD	Vanderbilt University Medical Center, Nashville, TN	Literature search, figures, data collection, analysis, writing of the manuscript
John H. Newman, MD	Vanderbilt University Medical Center, Nashville, TN	Data collection, analysis, writing of the manuscript
Rizwan Hamid, MD, PhD	Vanderbilt University Medical Center, Nashville, TN	Data collection, analysis, writing of the manuscript
Jens Meiler, PhD	Vanderbilt University Medical Center, Nashville, TN	Data collection, review final draft of the manuscript
John A. Capra, PhD	Vanderbilt University Medical Center, Nashville, TN	Data collection, review final draft of the manuscript
Jonathan H. Sheehan, PhD	Washington University in St. Louis, Missouri	Figures, data collection, analysis, writing of the manuscript
Francesco Vetrini, PhD	Indiana University School of Medicine, Indianapolis, IN	Figures, data collection, analysis, writing of the manuscript
Yaping Yang, PhD	Baylor College of Medicine, Houston, TX	Genetic data analysis, writing of the manuscript
Bonnie Black	Vanderbilt University Medical Center, Nashville, TN	Data collection, writing of the manuscript
Andr�e Diedrich, MD, PhD	Vanderbilt University Medical Center, Nashville, TN	Data collection, writing of manuscript, review paper
David Robertson, MD	Vanderbilt University Medical Center, Nashville, TN	Clinical evaluation, writing of the manuscript

Appendix (continued)

Name	Location	Contribution
Italo Biaggioni, MD	Vanderbilt University Medical Center, Nashville, TN	Clinical evaluation, writing of the manuscript, study design, genetic data analysis

References

- Skok VI. Nicotinic acetylcholine receptors in autonomic ganglia. *Auton Neurosci*. 2002;97(1-2):1-11.
- Yeh JJ, Yasuda RP, Davila-Garcia MI, et al. Neuronal nicotinic acetylcholine receptor alpha3 subunit protein in rat brain and sympathetic ganglion measured using a subunit-specific antibody: regional and ontogenic expression. *J Neurochem*. 2001;77(1):336-346.
- Grady SR, Moretti M, Zoli M, et al. Rodent habenulo-interpeduncular pathway expresses a large variety of uncommon nAChR subtypes, but only the alpha3beta4* and alpha3beta3beta4* subtypes mediate acetylcholine release. *J Neurosci*. 2009;29(7):2272-2282.
- Hernandez SC, Vicini S, Xiao Y, et al. The nicotinic receptor in the rat pineal gland is an alpha3beta4 subtype. *Mol Pharmacol*. 2004;66(4):978-987.
- Turner JR, Kellar KJ. Nicotinic cholinergic receptors in the rat cerebellum: multiple heteromeric subtypes. *J Neurosci*. 2005;25(40):9258-9265.
- Prato V, Taberner FJ, Hockley JRF, et al. Functional and molecular characterization of mechanoinsensitive "silent" nociceptors. *Cell Rep*. 2017;21(11):3102-3115.
- Vernino S, Low PA, Fealey RD, Stewart JD, Farrugia G, Lennon VA. Autoantibodies to ganglionic acetylcholine receptors in autoimmune autonomic neuropathies. *N Engl J Med*. 2000;343(12):847-855.
- Mukherjee S, Vernino S. Dysfunction of the pupillary light reflex in experimental autoimmune autonomic ganglionopathy. *Auton Neurosci*. 2007;137(1-2):19-26.
- Richardson CE, Morgan JM, Jasani B, et al. Megacystis-microcolon-intestinal hypoperistalsis syndrome and the absence of the alpha3 nicotinic acetylcholine receptor subunit. *Gastroenterology*. 2001;121(2):350-357.
- Mann N, Kause F, Henze EK, et al. CAKUT and autonomic dysfunction caused by acetylcholine receptor mutations. *Am J Hum Genet*. 2019;105(6):1286-1293.
- Xu W, Gelber S, Orr-Urtreger A, et al. Megacystis, mydriasis, and ion channel defect in mice lacking the alpha3 neuronal nicotinic acetylcholine receptor. *Proc Natl Acad Sci USA*. 1999;96(10):5746-5751.
- Sobreira N, Schiettecatte F, Valle D, Hamosh A. GeneMatcher: a matching tool for connecting investigators with an interest in the same gene. *Hum Mutat*. 2015;36(10):928-930.
- Mosqueda-Garcia R. Evaluation of autonomic failure. In: Robertson D, Biaggioni I, eds. *Disorders of the Autonomic Nervous System*. Harwood Academic Press; 1995:25-59.
- Low PA, Benarroch EE. *Clinical Autonomic Disorders*. Lippincott Williams & Wilkins; 2008.
- Diedrich A, Jordan J, Tank J, et al. The sympathetic nervous system in hypertension: assessment by blood pressure variability and ganglionic blockade. *J Hypertens*. 2003;21(9):1677-86.
- Goldstein DS, Polinsky RJ, Garty M, et al. Patterns of plasma levels of catechols in neurogenic orthostatic hypotension. *Ann Neurol*. 1989;26(4):558-563.
- Yang Y, Muzny DM, Xia F, et al. Molecular findings among patients referred for clinical whole-exome sequencing. *JAMA*. 2014;312(18):1870-1879.
- Lalani SR, Liu P, Rosenfeld JA, et al. Recurrent muscle weakness with rhabdomyolysis, metabolic crises, and cardiac arrhythmia due to Bi-allelic TANGO2 mutations. *Am J Hum Genet*. 2016;98(2):347-357.
- Gharpure A, Teng J, Zhuang Y, et al. Agonist selectivity and ion permeation in the alpha3beta4 ganglionic nicotinic receptor. *Neuron*. 2019;104(3):501-511.
- Kellogg EH, Leaver-Fay A, Baker D. Role of conformational sampling in computing mutation-induced changes in protein structure and stability. *Proteins*. 2011;79(3):830-838.
- Sivley RM, Dou X, Meiler J, Bush WS, Capra JA. Comprehensive analysis of constraint on the spatial distribution of missense variants in human protein structures. *Am J Hum Genet*. 2018;102(3):415-426.
- Sivley RM, Sheehan JH, Kropski JA, et al. Three-dimensional spatial analysis of missense variants in RTEL1 identifies pathogenic variants in patients with familial interstitial pneumonia. *BMC Bioinformatics*. 2018;19:18.
- Petersen EF, Goddard TD, Huang CC, et al. UCSF Chimera: a visualization system for exploratory research and analysis. *J Comput Chem*. 2004;25(13):1605-1612.
- Morin A, Eisenbraun B, Key J, et al. Collaboration gets the most out of software. *Elife*. 2013;2:e01456.
- Celedonio JE, Arnold AC, Dupont WD, et al. Residual sympathetic tone is associated with reduced insulin sensitivity in patients with autonomic failure. *Clin Auton Res*. 2015;25(5):309-315.
- Robertson D, Johnson GA, Robertson RM, Nies AS, Shand DG, Oates JA. Comparative assessment of stimuli that release neuronal and adrenomedullary catecholamines in man. *Circulation*. 1979;59(4):637-643.
- Walker LS, Stone AL, Smith CA, et al. Interacting influences of gender and chronic pain status on parasympathetically mediated heart rate variability in adolescents and young adults. *Pain*. 2017;158(8):1509-1516.

28. Singer W, Opfer-Gehrking TL, McPhee BR, Hilz MJ, Bharucha AE, Low PA. Acetylcholinesterase inhibition: a novel approach in the treatment of neurogenic orthostatic hypotension. *J Neurol Neurosurg Psychiatry*. 2003;74(9):1294-1298.
29. McCartney AC, Riordan-Eva P, Howes RC, Spalton DJ. Horner's syndrome: an electron microscopic study of a human iris. *Br J Ophthalmol*. 1992;76(12):746-749.
30. Caffery PM, Krishnaswamy A, Sanders T, et al. Engineering neuronal nicotinic acetylcholine receptors with functional sensitivity to alpha-bungarotoxin: a novel alpha3-knock-in mouse. *Eur J Neurosci*. 2009;30(11):2064-2076.
31. Xu W, Orr-Urtreger A, Nigro F, et al. Multiorgan autonomic dysfunction in mice lacking the beta2 and the beta4 subunits of neuronal nicotinic acetylcholine receptors. *J Neurosci*. 1999;19(21):9298-9305.
32. Taneja I, Robertson D. Genetic basis of autonomic dysfunction. *Semin Neurol*. 2003;23(1):391-397.
33. Robertson D, Goldberg MR, Onrot J, et al. Isolated failure of autonomic noradrenergic neurotransmission: evidence for impaired beta-hydroxylation of dopamine. *N Engl J Med*. 1986;314(23):1494-1497.
34. van den Berg MP, Almomani R, Biaggioni I, et al. Mutations in CYB561 causing a novel orthostatic hypotension syndrome. *Circ Res*. 2018;122(6):846-854.